Organic & Biomolecular Chemistry

Cite this: *Org. Biomol. Chem.*, 2011, **9**, 2667

www.rsc.org/obc

PAPER

Laccase-catalyzed phenol oxidation. Rapid assignment of ring-proton deficient polycyclic benzofuran regioisomers by experimental ^{1}H–^{13}C long-range coupling constants and DFT-predicted product formation†

Heiko Leutbecher,[a] Gerhard Greiner,[a] Robert Amann,[a] Andreas Stolz,[b] Uwe Beifuss*[a] and Jürgen Conrad*[a]

Received 4th January 2011, Accepted 1st February 2011
DOI: 10.1039/c1ob00012h

Laccase-catalyzed oxidation of substituted catechols followed by reaction with 4-hydroxy-pyrone/-benzopyrone afforded substituted benzofuran regioisomers whose structures with only two aromatic protons in total prevent a rapid structural assignment. Based on the evaluation of ^{1}H–^{13}C long-range coupling constants a rule of thumb could be deduced for an easy and unambiguous differentiation between the possible regioisomers formed. DFT frontier orbital calculations of the reactants offer an interesting tool to explain the regioselectivity of the key reaction.

Introduction

Natural compounds with a benzofuran skeleton are well known for their broad range of biological activities. Coumestans with a benzofuro[3,2-*c*]chromen-6-one structure are reported to exhibit phytoestrogenic, antibacterial, antifungal, antihepatotoxic and phytoalexin effects.[1] Pyrano[4,3-*b*]benzofuran-1-ones possess powerful antioxidant properties combined with a highly effective UV absorbing functionality making them interesting for cosmetic and dermatological formulations.[2] Oxidation of catechols *via* inorganic oxidants,[3a] electrochemically[3b] or enzymatically with tyrosinase[3c] followed by reaction with substituted 4-hydroxy-2*H*-pyran-2-one (**1a**) or 4-hydroxy-2*H*-chromen-2-one (**1b**) provides access to this class of interesting compounds. Very recently, we have found a simple and economical laccase-catalyzed domino reaction for the synthesis of such benzofurans and related structures (Scheme 1, Table 1).[4]

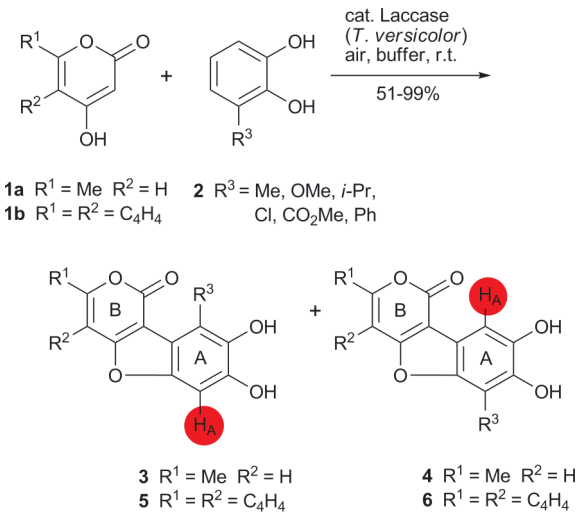

Scheme 1 Laccase-catalyzed synthesis of regioisomers **3–6**.

However, a major challenge comprises the rapid and unambiguous determination of the regioselectivity of the aforementioned reactions for the following reasons: many polyphenols suffer from a lack of aromatic protons in a way that classical NMR methods such as ^{1}H-NOE, ^{1}H-^{1}H-NOESY, ^{1}H-^{1}H-ROESY can only be applied to a certain extent—or not at all—for resolving stereochemical issues and/or regioselectivity. Even more, a limited sample amount or the absence of single crystals very often prevents ^{13}C–^{13}C correlations in NMR or X-ray analysis for an unambiguous assignment of the carbon skeleton, especially when looking at naturally occurring polyphenols. In those cases, derivatization reactions followed by time and solvent consuming work-up procedures as well as second NMR/X-ray analyses have to be performed. Other approaches to assign carbons in such protonless molecules rely on the prediction of ^{13}C NMR chemical shifts by quantum mechanical calculations and/or (semi)empirical methods using databases and/or incremental algorithms and subsequent comparison with experimental data.[5] Much research in this area is still being carried out with the focus on the improvement of the accuracy of such time-intensive computational calculations.[5] Nevertheless, the predicted chemical shifts could suffer from inaccuracy depending on the databases[6] or the applied calculation protocols.

[a]*Bioorganische Chemie, Institut für Chemie, Universität Hohenheim, Garbenstrasse 30, D-70599, Stuttgart, Germany. E-mail: juergen.conrad@uni-hohenheim.de; Fax: +49 711 459 22951; Tel: +49 711 459 22944*
[b]*Institut für Mikrobiologie, Universität Stuttgart, Allmandring 31, D-70569, Stuttgart, Germany. E-mail: andreas.stolz@imb.uni-stuttgart.de; Fax: +49 711 685 65725; Tel: +49 711 685 65489*

† Electronic supplementary information (ESI) available: Results of computational calculations, and ^{1}H and ^{13}C NMR spectra of all compounds. See DOI: 10.1039/c1ob00012h

Table 1 Laccase-catalyzed domino reaction of **1a** or **1b**, respectively, and **2a–f**

Entry	1	2	R^3	Time (h)	Product(s)	Yield (%)
1	**a**	**a**	Me	3	**4a**	99
2	**a**	**b**	OMe	4.5	**4b**	51
3	**a**	**c**	*i*-Pr	4	**4c**	93
4	**a**	**d**	Cl	6	**3d**	67
5	**a**	**e**	CO_2Me	4	**3e**, **7**[a]	85
6	**a**	**f**	Ph	6	**3f**, **4f**[b]	94
7	**b**	**a**	Me	3	**6a**	99
8	**b**	**b**	OMe	5	**6b**	61
9	**b**	**e**	CO_2Me	4	**5e**, **8**[c]	89

[a] **3e** is accompanied by pyrano[4,3-*c*]isochromen-1,6-dione **7** (**3e** : **7** = 7 : 3) (Fig. 1). [b] **3f** and **4f** were obtained in a 1 : 4.1 ratio. [c] **5e** is accompanied by isochromeno[4,3-*c*]chromen-6,11-dione **8** (**5e** : **8** = 7.1 : 2.9) (Fig. 1).

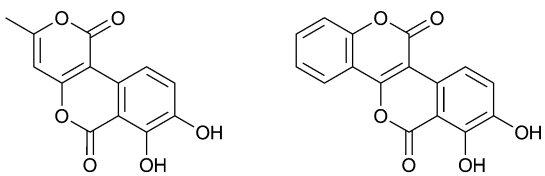

7 **8**

Fig. 1 Side products **7** and **8** from domino reaction of **2e** and **1a** or **1b**, respectively.

In this work we present (i) an experimental methodology for the rapid differentiation of the synthesized regioisomers based on the evaluation of experimental ^1H–^{13}C long-range coupling constants and demonstrate that (ii) DFT frontier orbital calculations of the reactants may offer a promising tool for the explanation of the regioselectivity of such reactions.

Results and discussion

For our studies of the regioselectivity of the laccase-catalyzed domino reaction we prepared in total ten pyrano[4,3-*b*]benzofuran-1-ones and benzofuro[3,2-*c*]chromen-6-ones, four of them (**4c**, **3d**, **3f** and **4f**) being new compounds (Table 1). The synthesis of **3e**, **5e**, **7** and **8** has already been published by Leutbecher *et al.* elsewhere.[4a]

In most cases the domino reaction delivers only one of two possible regioisomers. However, the ring-proton deficiency in the products did not allow a rapid structural assignment by standard NMR methods. Considering, for example, regioisomers **3** and **4**, only one proton represents aromatic ring A and another proton ring B. In such cases, a common gHMBC optimized for J_{CH} = 8 Hz provides a series of $^2J_{CH}$–$^4J_{CH}$ long-range correlations. In compound **4a**, the aromatic proton H_A (δ 7.06 ppm) shows four correlations with ring A carbons at δ_C 112.31, 143.36, 143.78 and 148.09 ppm. Due to missing additional aromatic protons in ring A, those values can not be assigned to the respective positions in the ring system. Consequently, the substitution pattern of ring A and the connectivity with the remaining subunit B—thus fixing the regioselectivity—can not be determined. Unfortunately, in most NMR solvents the phenolic protons very often appear not as sharp singlets but as broad humps which show no ^1H–^{13}C long-range correlations for assignment purposes at all. To circumvent derivatization reactions such as methylation and avoiding time and solvent consuming work-up procedures along with a second NMR analysis, we applied different computational methods for the prediction of ^{13}C NMR chemical shifts including quantum mechanical DFT calculations and (semi)empirical methods using databases and/or incremental algorithms (ACD/Labs).[5,7] For evaluation of this approach we calculated the ^{13}C NMR chemical shifts of the regioisomers **4a**, **3d**, **3f** and **4f** and compared them with the experimental data. The ring A carbons of **4a** (see above), for instance, were calculated at the DFT GIAO B3LYP/6-311+G(2d,p)//B3LYP/6-31G(d) level of theory[8] to be at δ_C 120.47, 149.05, 151.23 and 156.01 ppm with TMS as reference compound. By an MSTD approach published only recently,[9] comprising benzene as a reference for sp^2 carbons the aforementioned chemical shifts were recalculated at δ_C 114.19, 142.77, 144.95 and 149.73 ppm which match the experimental values much better than the calculation with TMS as reference. The MSTD method with benzene and the mPW1PW91/6-311+G(2d,p)//mPW1PW91/6-31G(d) level of theory[9] resulted in δ_C 113.03, 141.30, 143.30 and 147.67 ppm for the ring A carbons, already close to the experimental data. For comparison, the predicted chemical shifts by ACD/Labs[7] were at δ_C 118.43, 143.73, 145.93 and 156.61 ppm. Similar consistency between the experimental and calculated data was observed for **3d**: $\delta_{C(exp.)}$ 112.83, 141.12, 146.19 and 147.77 ppm and $\delta_{C(calc.)}$ 114.51, 140.30, 146.56 and 150.46 (B3LYP/6-311+G(2d,p)//B3LYP/6-31G(d)). When comparing the experimental ^{13}C NMR chemical shifts of the ring A carbons of **3f** (δ_C 112.92, 141.26, 145.14, 147.82 ppm) and **4f** (δ_C 113.01, 142.56, 144.29, 146.68 ppm), only small shift differences of up to 1.3 ppm were detected. Deviations of up to 3 ppm between the experimental and calculated chemical shifts of these carbons, both in **3f** ($\delta_{C(calc.)}$ 112.74, 138.40, 145.09, 149.01 ppm) and **4f** ($\delta_{C(calc.)}$ 115.84, 138.99, 145.44, 147.37 ppm) at the mPW1PW91/6-311+G(2d,p)//mPW1PW91/6-31G(d) level, unfortunately did not support any assignment and thus did not allow a differentiation of those regioisomers. A better accuracy would probably be achieved by additional diffuse and polarization functions and/or another basis set such as Aug-CC-pVTZ,[8] but at the expense of much higher computational costs.

In the search for more rapid and direct solutions we have found and evaluated a methodology based on experimental ^1H–^{13}C long-range coupling constants for the unambiguous determination of such regioisomers independently from ^{13}C NMR chemical shift considerations. We used the HSQMBC pulse sequence for the rapid and accurate determination of the ^1H–^{13}C long-range coupling constants of all compounds.[10] The ^1H–^{13}C long-range coupling constants between H_A and the ring A carbons C-9a, C-5a, C-7 and C-8 were found to be highly consistent within each set of regioisomers **3** and **4** despite ^{13}C chemical shift differences for those carbons due to different substitution patterns (Fig. 2). Since $^3J_{CH}$ coupling constants in those aromatic ring systems are significantly greater (absolute values between 4 and 12 Hz) than $^2J_{CH}$ and $^4J_{CH}$ coupling constants, the carbons with smaller coupling constants (*e.g.* **4a**: absolute values of $^2J_{CH}$ = 2.1 and 3.1 Hz)[11] were assigned as the carbons at both *ortho*-positions (C-9a and C-8) and the carbons with larger coupling constants (*i.e.* **4a**: absolute values of $^3J_{CH}$ = 7.5 and 10.4 Hz) to both *meta*-positions (C-7 and C-5a) with respect to H_A.

Compared to regioisomers **4**, the extracted ^1H–^{13}C long-range coupling constants between H_A and the respective carbons

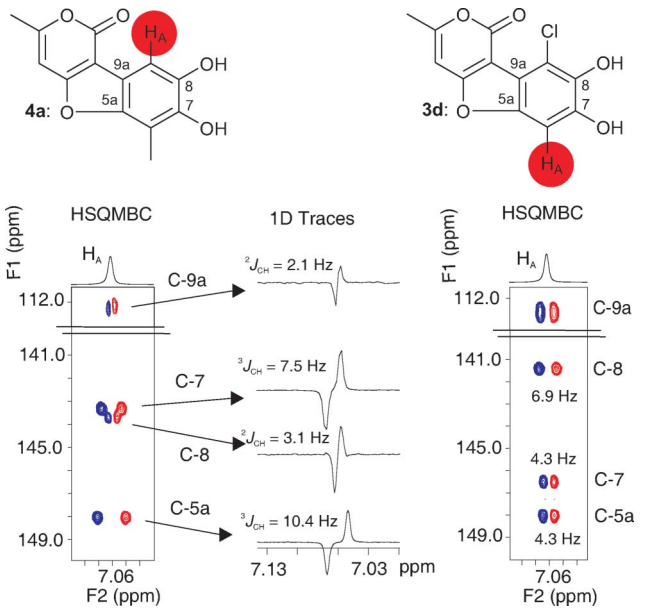

Fig. 2 ^{1}H–^{13}C long-range couplings of H_A of **4a** and **3d** to ring A carbons, measured by HSQMBC.

C-5a, C-7, C-8 as well as C-9a differed considerably in size of regioisomers **3**, *e.g.* **3d**: $J_{C\text{-}5aH_A}$ = 4.3 Hz, $J_{C\text{-}7H_A}$ = 4.3 Hz, $J_{C\text{-}8H_A}$ = 6.9 Hz, $J_{C\text{-}9aH_A}$ = 5.7 Hz. However, as both coupling patterns were almost constant within each set of regioisomers **3** and **4** (Table 2), the following rule could be deduced: ^{1}H–^{13}C long-range coupling constants of $J_{CH} \approx$ 4.3, 4.3, 6.7 and 5.5 Hz to ring A carbons C-5a, C-7, C-8 and C-9a (Scheme 1, Table 2) establish the structures of products **3**, whereas two big coupling constants of $J_{CH} \approx$ 10.4 and 7.3 and a small one of $J_{CH} \approx$ 3.0 Hz to the oxygen bearing carbons C-5a, C-7 and C-8 (Scheme 1, Table 2) indicate the chemical structures of **4** for these types of compounds.

In order to verify and broaden its applicability we tested the rule on the determination of the regioisomers **5** and **6** obtained by laccase-catalyzed domino reaction of catechols **2** with 4-hydroxy-2*H*-chromen-2-one (**1b**) (Scheme 1, Fig. 3) and found, again, J_{CH} coupling constant patterns for the two regioisomers nearly identical to **3** and **4** (Table 2).

Table 2 Experimental ^{1}H–^{13}C long-range coupling constants of H_A to ring A carbons of **3** and **4** as well as **5** and **6**

Entry	Compound	C-5a[a]	C-7[a]	C-8[a]	C-9a[a]
1	**3d**[b]	4.3 (5.5)	4.3 (4.5)	6.9 (6.2)	5.7 (4.7)
2	**3e**	4.4	4.4	6.5	5.7
3	**3f**[b]	4.4 (5.2)	4.2 (5.4)	6.5 (6.3)	5.4 (4.8)
4	**4a**[b]	10.4 (9.0)	7.5 (6.7)	3.1 (3.3)	2.1 (2.2)
5	**4b**	10.4	7.4	2.9	1.9
6	**4c**	10.3	7.4	2.8	1.8
7	**4f**[b]	10.2 (9.5) C-10a[a]	7.4 (7.0) C-9[a]	2.9 (4.5) C-8[a]	1.9 (1.4) C-6b[a]
8	**5e**	4.5	4.2	6.6	5.8
9	**6a**	10.3	7.4	3.0	2.5
10	**6b**	10.2	7.5	2.8	2.0

[a] J_{CH} in Hz (absolute values). [b] DFT-calculated J_{CH} of **3d**, **4a**, **3f** and **4f** in parentheses (mPW1PW91/6-311+G(2d,p)//mPW1PW91/6-31G(d)).

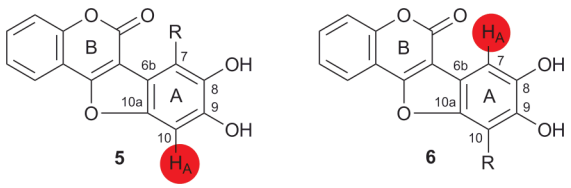

Fig. 3 Products **5** and **6** from domino reaction of **1b** and **2**.

Even more, this approach can successfully be exploited for the fast analysis of mixtures of regioisomers *e.g.* **3f** and **4f** obtained as a 1 : 4.1 mixture. Two big and only one small coupling constants to oxygen bearing aromatic carbons (10.2, 7.4, 2.9 Hz) establish structure **4f** as the major whereas coupling constants of J_{CH} = 4.2, 4.4, 5.4 and 6.5 Hz indicate **3f** as the minor component (Fig. 4).

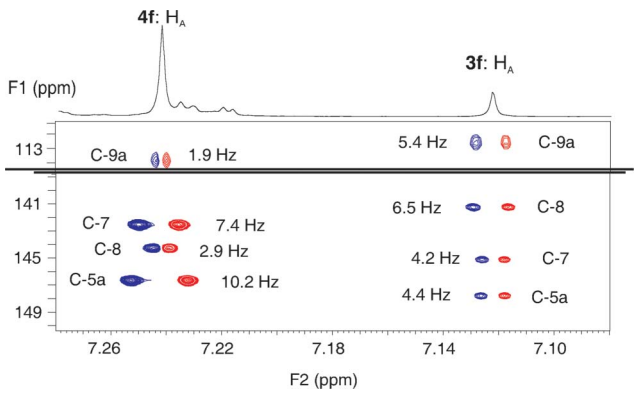

Fig. 4 Expansion of the HSQMBC of a 1 : 4.1 mixture of **3f** and **4f**. J_{CH} coupling constants (absolute values) between H_A and ring A carbons are shown.

Similarly to the ^{13}C NMR considerations we calculated the ^{1}H–^{13}C long-range coupling constants of **3d**, **4a**, **3f** and **4f** at the mPW1PW91/6-311+G(2d,p)//mPW1PW91/6-31G(d) level of theory to evaluate their suitability for assignment purposes of the investigated molecules. Comparison with the experimental data (Table 2, entries 1, 3, 4 and 7) reveals that the calculated values follow the patterns observed for **3** and **4** despite deviations of up to 1.6 Hz between the experimental and calculated data. Thus, the calculation of ^{1}H–^{13}C long-range coupling constants seems to be a much better option for the differentiation of the regioselectivity than the ^{13}C chemical shift considerations. However, the accurate determination of coupling constants requires tremendous computational time (*e.g.* **4f**: 108 h) in addition to the recording of an HSQMBC NMR spectrum (*e.g.* **4f**: 8 h).

In addition to the fast and direct NMR based determination of the regioselectivity we have also searched for theoretical alternatives to the time-intensive DFT GIAO ^{13}C NMR approach and performed DFT frontier orbital calculations of the reactants at the B3LYP/6-31G(d) level for the prediction of the regioisomers formed.[4c–d,12] Consideration of the frontier orbital energies of **1a** and of reaction intermediate **9** revealed a smaller energy difference between the HOMO of **1a** and LUMOs of **9** than between the LUMO of **1a** and HOMOs of **9** (Table 3). Thus, a nucleophilic attack of 2*H*-pyran-2-one **1a** on quinones **9** could be expected.

The softer nucleophilic center, *e.g.* the carbon atom of the enol of **1a** (atomic orbital coefficients of the enol: oxygen –0.285, carbon 0.553), should react with the most electrophilic center of quinones

Table 3 Frontier orbital energies of **9a–f** and **1a**

Entry	Compound	R	HOMO (eV)	LUMO (eV)
1	**9a**	Me	–6.69	–3.46
2	**9b**	OMe	–6.29	–3.43
3	**9c**	*i*-Pr	–6.67	–3.42
4	**9d**	Cl	–7.16	–3.86
5	**9e**	CO_2Me	–7.05	–4.03
6	**9f**	Ph	–6.44	–3.49
7	**1a**		–6.15	–1.18

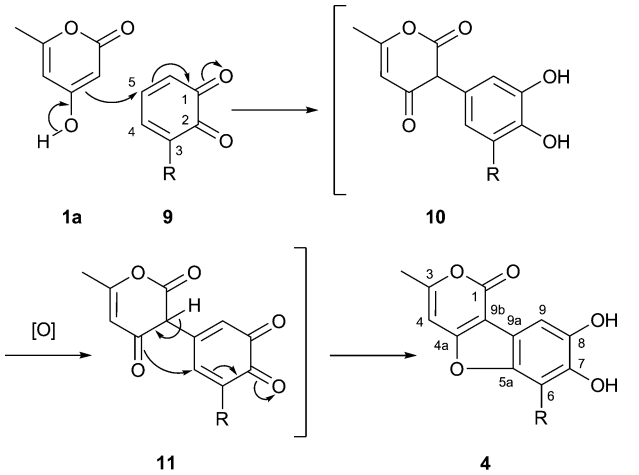

Scheme 2 Proposed mechanism of the laccase-catalyzed domino reaction.

9 (Scheme 2). That is the carbon atom with the largest atomic orbital coefficient, C-4 or C-5, respectively.

As shown in Fig. 5, quinones **9a**, **9b** and **9c** have their largest atomic orbital coefficients at C-5. According to expectations, regioisomers **4a**, **4b** and **4c** are the exclusive products of the domino reaction between **1a** and **2a**, **2b** and **2c** (Table 1). C-4 of **9d** and **9e** should be the preferred position for the nucleophilic attack of **1a**. The experimental results are also in excellent agreement with the DFT-calculations (Table 1). Only the reaction of **1a** with **2f** leads to a mixture of regioisomers **3f** and **4f** (Table 1), which is probably due to the steric hindrance caused by the bulky phenyl substituent during the first step of the reaction.[13] A preferred attack of **1a** onto the less hindered carbon atom C-5 of **9f** can be observed. Presumably, in addition to the electronic properties of

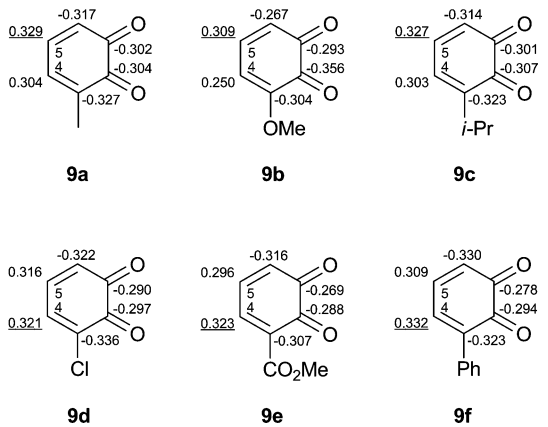

Fig. 5 Atomic orbital coefficients of LUMOs of **9a–f**.

the nucleophile and the quinones, other effects, *e.g.* steric factors, must be involved and influence the reaction kinetics.[12,13]

Conclusions

In conclusion, we have synthesized and analyzed the regioisomers formed by the laccase-catalyzed domino reaction of catechols and substituted 4-hydroxy-2*H*-pyran-2-one (**1a**) or 4-hydroxy-2*H*-chromen-2-one (**1b**). During these studies we have found a rapid and elegant methodology for the unequivocal determination of the regioselectivity of those reactions yielding ring-proton deficient products based on experimental ^{1}H–^{13}C long-range coupling constants which were partially corroborated by time-intensive DFT GIAO calculations. Furthermore, frontier orbital consideration of the intermediates seems to be a valuable tool for the explanation of the regioselectivity of those reactions. Overall, we are convinced that both strategies—(i) experimental ^{1}H–^{13}C long-range coupling constants and (ii) frontier orbital consideration—can be easily and successfully exploited for a much wider range of even more complicated molecules avoiding quite often painstaking and time consuming identification procedures.

Experimental

Computational studies

All the calculations reported in this paper were performed within Density Functional Theory, using the Gaussian 03 package.[8] Frontier orbital energies were calculated at the B3LYP/6-31G(d) level of theory. Atomic orbital coefficients of frontier orbitals were obtained using the STO-3G basis set. ^{13}C NMR chemical shifts of selected compounds **3d**, **4a**, **3f** and **4f** were calculated as follows: The rigid structures were optimized with the MM2 force field implemented in Chem3D Pro.[14] In the second step, the optimized structures were subsequently reoptimized at the AM1 level followed by the RHF/3-21G level and finally by the B3LYP/6-31G(d) level of theory within the Gaussian 03 package. In the final step, the ^{13}C NMR chemical shifts of the reoptimized geometries were computed once at the B3LYP/6-311+G(2d,p)//B3LYP/6-31G(d) level of theory and twice at the mPW1PW91/6-311+G(2d,p)//mPW1PW91/6-31G(d) level of theory using the IEFPCM model of solvation and DMSO as solvent in both calculations.[8] The references TMS and benzene for the MSTD approach according to Sarotti and Pellegrinet[9] were computed in the same manner as for **3d**, **4a**, **3f** and **4f**. For comparison the ^{13}C NMR chemical shifts were predicted using ACD/CNMR Predictor.[7] The ^{1}H–^{13}C long-range coupling constants between H_A and the ring A carbons of **3d**, **4a**, **3f** and **4f** were calculated at the mPW1PW91/6-311+G(2d,p)//mPW1PW91/6-31G(d) level of theory using the IEFPCM model and DMSO as solvent. An HP Compaq with a 2.39 GHz processor and 2 GB RAM was used for the calculations.

Determination of laccase activity

The activity of commercially available laccase (EC 1.10.3.2) from *Trametes versicolor* (Fluka, Buchs) was determined following a procedure taken from Nicotra *et al.*[15] A solution of ABTS (0.3 mL; 51.61 mg ABTS in 10 mL of 0.2 M acetate buffer, pH = 4.4) was diluted with 0.2 M acetate buffer (2.67 mL, pH = 4.4) and

treated with a solution of laccase in the same buffer (0.03 mL). The change in absorption was followed *via* UV-spectroscopy (λ = 414 nm). One unit was defined as the amount of laccase that converts 1 μmol of ABTS per minute at pH = 4.4 at room temperature.

General

Commercial reagents were used without further purification. Thin-layer chromatography (TLC) was performed on silica gel SIL G/UV_{254} (Macherey-Nagel); compounds were visualized with UV light (λ = 254 nm) and/or immersion in vanillin/H_2SO_4 solution followed by heating. Melting points were determined on a Kofler melting point apparatus (Reichert) and are uncorrected. UV/Vis spectra were measured using a CARY 4E (Varian). IR (atr) spectra were taken on a Spectrum One (Perkin Elmer). NMR spectra were recorded on a Varian ^{Unity}INOVA spectrometer (500/125 MHz) in DMSO-d_6; the ^{1}H and ^{13}C chemical shifts were referenced to residual solvent signals at δ_H = 2.49 and δ_C = 39.5 (DMSO) relative to TMS. *J* values are given in Hz. All 1D (^{1}H, ^{13}C) and 2D NMR (COSY, ROESY, gHSQCAD, gHMBCAD) measurements were performed using standard pulse sequences. HSQMBC parameters: sw = 4000–6000 Hz, sw1 = 8000–12 000 Hz, np = 8192, fn = 16 384, jnxh = 8, ni = 128–512, nt = 16–64, d1 = 1. Linear Prediction in F1. Mass spectra (EI) were recorded on a MAT 95 (Finnigan MAT) with 70 eV ionization energy.

General procedure for the synthesis of 7,8-dihydroxy-1*H*-pyrano[4,3-*b*]benzofuran-1-ones 3 and 4, and 8,9-dihydroxy-6*H*-benzofuro[3,2-*c*]chromen-6-ones 5 and 6

4-Hydroxy-6-methyl-2*H*-pyran-2-one (**1a**) (378 mg, 3.0 mmol) or 4-hydroxy-2*H*-chromen-2-one (**1b**) (491 mg, 3.0 mmol), respectively, and catechol **2a**, **2b** and **2e** (3.3 mmol), respectively, were dissolved in acetate buffer (200 mL, pH = 4.4, 0.2 M) and vigorously stirred under air at r.t. in the presence of 475 U laccase of *T. versicolor* until the substrates had been fully consumed, as judged by TLC. The reaction mixture was saturated with NaCl and filtered on a Buchner funnel. The filter cake was washed with a solution of 15% NaCl (200 mL) and water (10 mL). The crude products obtained after drying exhibited a purity of 90–95% (NMR). Analytically pure products could be obtained by recrystallization.

Transformations of **1a** (0.5 mmol) and **2c** or **2d** (0.55 mmol), respectively, were performed in acetate buffer (70 mL) on a smaller scale. Reaction of **1a** (0.45 mmol) and **2f** (0.5 mmol) was performed in a buffer/acetone mixture (85 mL, *v*/*v* = 16 : 1).

7,8 -Dihydroxy-3,6-dimethyl-1*H*-pyrano[4,3-*b*]benzofuran-1-one (4a). Brown solid, 99% yield; mp >300 °C (dec.) (lit.,[3b] 257–259 °C, dec.); δ_H(500 MHz; DMSO-d_6) 2.28 (3 H, s, 6-CH_3), 2.32 (3 H, br s, 3-CH_3), 6.86 (1 H, br s, 4-H), 7.06 (1 H, s, 9-H), 8.74 (1 H, br s, OH), 9.63 (1 H, br s, OH); δ_C(125 MHz; DMSO-d_6) 8.93 (6-CH_3), 19.81 (3-CH_3), 95.91 (C-4), 101.69 (C-9), 103.11 (C-9b), 108.37 (C-6), 112.31 (C-9a), 143.36 (C-7), 143.78 (C-8), 148.09 (C-5a), 158.99 (C-1), 161.06 (C-3), 162.91 (C-4a); *m*/*z*(EI, 70 eV) 246 (M^+, 100%), 231 ($M^+ - CH_3$, 11), 217 (13), 203 (5), 190 (3), 176 (7), 147 (2), 123 (5), 43 (24).

7,8-Dihydroxy-6-methoxy-3-methyl-1*H*-pyrano[4,3-*b*]benzofuran-1-one (4b). Brown solid, 51% yield; mp 230–234 °C (dec.) (lit.,[3b] 225–227 °C, dec.); δ_H(500 MHz; DMSO-d_6) 2.33 (3 H, br s, 3-CH_3), 3.97 (3 H, s, OCH_3), 6.92 (1 H, br s, 4-H), 6.93 (1 H, s, 9-H), 8.96 (1 H, br s, OH), 9.50 (1 H, br s, OH); δ_C(125 MHz; DMSO-d_6) 19.81 (3-CH_3), 60.52 (OCH_3), 95.88 (C-4), 99.17 (C-9), 102.92 (C-9b), 113.58 (C-9a), 133.54 (C-6), 137.42 (C-7), 140.82 (C-5a), 145.46 (C-8), 158.88 (C-1), 161.54 (C-3), 163.16 (C-4a); *m*/*z*(EI, 70 eV) 262 (M^+, 100%), 247 ($M^+ - CH_3$, 44), 233 (2), 219 (5), 205 (3), 191 (3), 163 (2), 146 (2), 131 (M^{2+}, 5), 43 (31).

7,8-Dihydroxy-6-isopropyl-3-methyl-1*H*-pyrano[4,3-*b*]benzofuran-1-one (4c). Brown solid, 93% yield; mp 259–261 °C (from ethyl acetate, dec.); λ_{max}(MeOH)/nm 245 (lg ε 4.23), 333 (4.17); $\tilde{\nu}_{max}$(atr)/cm^{-1} 3553 and 2961 (OH), 1736 (C═O), 1611 and 1569 (C═C), 1382 (CH_3), 1294 (OH), 1213 and 1041 (C–O), 854 (═C–H); δ_H(500 MHz; DMSO-d_6) 1.35 (6 H, d, $^3J_{(CH_3)_2,(CH_3)_2CH}$ 7.1, (CH_3)$_2$CH), 2.34 (3 H, br s, 3-CH_3), 3.56 (1 H, sept, $^3J_{(CH_3)_2CH,(CH_3)_2}$ 7.1, (CH_3)$_2$C*H*), 6.93 (1 H, br s, 4-H), 7.08 (1 H, s, 9-H), 8.60 (1 H, br s, OH), 9.76 (1 H, br s, OH); δ_C(125 MHz; DMSO-d_6) 19.81 (3-CH_3), 21.08 [(CH_3)$_2$], 24.85 [*C*H(CH_3)$_2$], 95.96 (C-4), 101.74 (C-9), 102.82 (C-9b), 112.97 (C-9a), 118.76 (C-6), 142.57 (C-7), 143.86 (C-8), 147.47 (C-5a), 158.98 (C-1), 161.14 (C-3), 162.74 (C-4a); *m*/*z*(EI, 70 eV) 274.0818 (M^+, 100%. $C_{15}H_{14}O_5$ requires 274.0842), 259 ($M^+ - CH_3$, 95), 231 (5), 213 (5), 203 (4), 185 (3), 137 (M^{2+}, 2), 129 (5), 99 (3), 43 (9).

9-Chloro-7,8-dihydroxy-3-methyl-1*H*-pyrano[4,3-*b*]benzofuran-1-one (3d). White solid, 67% yield; mp >300 °C (dec.); λ_{max}(MeCN)/nm 227 (lg ε 4.28), 328 (4.22); $\tilde{\nu}_{max}$(atr)/cm^{-1} 3575 and 3209 (OH), 1733 (C═O), 1618, 1564 and 1490 (C═C), 1380 (OH), 1221 (C–O), 1037 (C–O or C–Cl), 849 (═C–H); δ_H(500 MHz; DMSO-d_6) 2.32 (3 H, s, 3-CH_3), 6.84 (1 H, s, 4-H), 7.06 (1 H, s, 6-H), 9.18 (1 H, br s, OH), 10.29 (1 H, br s, OH); δ_C(125 MHz; DMSO-d_6) 19.68 (3-CH_3), 95.33 (C-4), 97.24 (C-6), 102.29 (C-9b), 111.69 (C-9), 112.83 (C-9a), 141.12 (C-8), 146.19 (C-7), 147.77 (C-5a), 156.99 (C-1), 162.30 (C-3), 163.77 (C-4a); *m*/*z*(EI, 70 eV) 265.9941 (M^+, 85%. $C_{12}H_7ClO_5$ requires 265.9982), 251 ($M^+ - CH_3$, 25), 237 (8), 233 (4), 196 (8), 133 (3), 43 (23).

7,8-Dihydroxy-3-methyl-1-oxo-1*H*-pyrano[4,3-*b*]benzofuran-9-carboxylic acid methyl ester (3e). White solid, 60% yield; t_R/min 8 (HPLC on Phenomenex Aqua RP-18 250 × 10 mm column, 5 μm, 30% MeCN (0.01% TFA), flow rate of 4 mL min^{-1}); mp 237–239 °C (dec.); λ_{max}(MeCN)/nm 233 (lg ε 4.28), 335 (4.18); $\tilde{\nu}_{max}$(atr)/cm^{-1} 3405 and 3119 (OH), 1703 (C═O), 1440 (CH_3), 1296 (OH), 1220 and 1050 (C–O), 839 (═C–H); δ_H(500 MHz; DMSO-d_6) 2.33 (3 H, s, 3-CH_3), 3.81 (3 H, s, OCH_3), 6.91 (1 H, s, 4-H), 7.17 (1 H, s, 6-H); δ_C(125 MHz; DMSO-d_6) 19.75 (3-CH_3), 51.68 (OCH_3), 95.59 (C-4), 99.29 (C-6), 102.26 (C-9b), 110.19 (C-9a), 113.69 (C-9), 141.27 (C-8), 145.64, 147.68 (C-5a or C-7), 157.96 (C-1), 162.00 (C-3), 163.55 (C-4a), 165.97 (*C*O_2CH_3); *m*/*z*(EI, 70 eV) 290.0425 (M^+, 20%. $C_{14}H_{10}O_7$ requires 290.0427), 258 ($M^+ - CH_4O$, 100), 229 (4), 202 (16), 174 (11), 69 (7), 43 (19).

7,8-Dihydroxy-3-methyl-6-phenyl-1*H*-pyrano[4,3-*b*]benzofuran-1-one (4f). Brown solid, 76% yield; mp 262–264 °C (from $CHCl_3$, dec.); λ_{max}(MeOH)/nm 251 (lg ε 4.44), 335 (4.19); $\tilde{\nu}_{max}$(atr)/cm^{-1} 3495 and 3057 (OH), 1736 (C═O), 1616, 1570 and 1493 (C═C), 1308 (OH), 1238 and 1043 (C–O), 885, 764 and 695 (═C–H); δ_H(500 MHz; DMSO-d_6) 2.32 (3 H, s, 3-CH_3), 6.89 (1 H, br s, 4-H), 7.24 (1 H, s, 9-H), 7.38 (1 H, t, $^3J_{4'-H,3'-H}$ = $^3J_{4'-H,5'-H}$ 7.4, 4′-H), 7.47 (2 H, t, $^3J_{3'-H,2'-H}$ = $^3J_{3'-H,4'-H}$ = $^3J_{5'-H,4'-H}$ = $^3J_{5'-H,6'-H}$ 7.6, 3′-

H, 5′-H), 7.59 (2 H, d, $^3J_{2'\text{-H},3'\text{-H}} = {}^3J_{6'\text{-H},5'\text{-H}}$ 7.7, 2′-H, 6′-H), 8.83 (1 H, s, 7-OH), 9.99 (1 H, s, 8-OH); δ_C(125 MHz; DMSO-d_6) 19.83 (3-CH_3), 95.95 (C-4), 102.93 (C-9b), 103.28 (C-9), 113.01 (C-9a), 113.42 (C-6), 127.42 (C-4′), 128.01 (C-3′, C-5′), 130.25 (C-2′, C-6′), 132.09 (C-1′), 142.56 (C-7), 144.29 (C-8), 146.68 (C-5a), 158.93 (C-1), 161.30 (C-3), 163.12 (C-4a); *m*/*z*(EI, 70 eV) 308.0687 (M^+, 100%. $C_{18}H_{12}O_5$ requires 308.0685), 293 ($M^+ - CH_3$, 5), 279 (7), 237 (9), 181 (3), 152 (4), 43 (4).

7,8-Dihydroxy-3-methyl-9-phenyl-1*H*-pyrano[4,3-*b*]benzofuran-1-one (3f). NMR-spectroscopic data of **3f** were deduced from the mixture of **3f** and **4f**. Only **4f** could be isolated in pure form by recrystallization from $CHCl_3$.

δ_H(500 MHz; DMSO-d_6) 2.26 (3 H, s, 3-CH_3), 6.82 (1 H, br s, 4-H), 7.12 (1 H, s, 6-H), 7.23 (2 H, m, 2′-H, 6′-H), 7.29 (3 H, m, 3′-H, 4′-H, 5′-H), 8.14 (1 H, s, 8-OH), 10.17 (1 H, s, 7-OH); δ_C(125 MHz; DMSO-d_6) 19.61 (3-CH_3), 95.25 (C-4), 97.22 (C-6), 102.49 (C-9b), 112.92 (C-9a), 126.52 (C-4′), 126.65 (C-3′, C-5′), 130.61 (C-2′, C-6′), 136.04 (C-1′), 141.26 (C-8), 145.14 (C-7), 147.82 (C-5a), 156.60 (C-1), 161.28 (C-3), 163.47 (C-4a).

8,9-Dihydroxy-10-methyl-6*H*-benzofuro[3,2-*c*]chromen-6-one (6a). Brown solid, 99% yield; mp >300 °C (dec.) (lit.,[16] 304–306 °C, dec.); δ_H(500 MHz; DMSO-d_6) 2.36 (3 H, s, 10-CH_3), 7.15 (1 H, s, 7-H), 7.42 (1 H, ddd, $^3J_{2\text{-H},1\text{-H}} = {}^3J_{2\text{-H},3\text{-H}}$ 7.5, $^4J_{2\text{-H},4\text{-H}}$ 1.0, 2-H), 7.50 (1 H, dd, $^3J_{4\text{-H},3\text{-H}}$ 8.1, $^4J_{4\text{-H},2\text{-H}}$ 0.9, 4-H), 7.61 (1 H, ddd, $^3J_{3\text{-H},2\text{-H}}$ 7.2, $^3J_{3\text{-H},4\text{-H}}$ 8.4, $^4J_{3\text{-H},1\text{-H}}$ 1.6, 3-H), 7.94 (1 H, dd, $^3J_{1\text{-H},2\text{-H}}$ 7.7, $^4J_{1\text{-H},3\text{-H}}$ 1.6, 1-H); δ_C(125 MHz; DMSO-d_6) 8.98 (10-CH_3), 101.86 (C-7), 105.64 (C-6a), 108.53 (C-10), 112.41 (C-11b), 112.95 (C-6b), 116.98 (C-4), 121.10 (C-1), 124.81 (C-2), 131.14 (C-3), 144.17 (C-8), 144.22 (C-9), 149.03 (C-10a), 152.25 (C-4a), 157.52 (C-6), 157.58 (C-11a); *m*/*z*(EI, 70 eV) 282 (M^+, 100%), 265 (<1), 253 (1), 208 (2), 141 (M^{2+}, 7), 115 (2).

8,9-Dihydroxy-10-methoxy-6*H*-benzofuro[3,2-*c*]chromen-6-one (6b). Brown solid, 61% yield; mp 236–238 °C (from ethanol/water, dec.) (lit.,[16] 260–261 °C, dec.); δ_H(500 MHz; DMSO-d_6) 4.08 (3 H, s, OCH_3), 7.05 (1 H, s, 7-H), 7.46 (1 H, pt, $^3J_{2\text{-H},1\text{-H}} = {}^3J_{2\text{-H},3\text{-H}}$ 7.7, 2-H), 7.55 (1 H, d, $^3J_{4\text{-H},3\text{-H}}$ 8.4, 4-H), 7.64 (1 H, ddd, $^3J_{3\text{-H},2\text{-H}}$ 7.4, $^3J_{3\text{-H},4\text{-H}}$ 8.6, $^4J_{3\text{-H},1\text{-H}}$ 1.7, 3-H), 8.03 (1 H, dd, $^3J_{1\text{-H},2\text{-H}}$ 7.9, $^4J_{1\text{-H},3\text{-H}}$ 1.7, 1-H), 9.13 (1 H, br s, OH), 9.64 (1 H, br s, OH); δ_C(125 MHz; DMSO-d_6) 61.34 (OCH_3), 100.04 (C-7), 106.24 (C-6a), 113.02 (C-11b), 114.95 (C-6b), 117.78 (C-4), 122.04 (C-1), 125.63 (C-2), 132.18 (C-3), 134.36 (C-10), 138.83 (C-9), 142.44 (C-10a), 146.58 (C-8), 153.09 (C-4a), 158.19 (C-11a), 158.68 (C-6); *m*/*z*(EI, 70 eV) 298 (M^+, 100%), 283 ($M^+ - CH_3$, 52), 255 (20), 237 (2), 171 (3), 149 (M^{2+}, 6), 115 (5).

8,9-Dihydroxy-6-oxo-6*H*-benzofuro[3,2-*c*]chromen-7-carboxylic acid methyl ester (5e). White solid, 63% yield; t_R/min 15 (HPLC on Phenomenex Aqua RP-18 250 × 10 mm column, 5 µm, 42% MeCN (0.01% TFA), flow rate of 4 mL min^{-1}); mp 244–246 °C (dec.); λ_{max}(MeCN)/nm 210 (lg ε 4.62), 239 (4.25), 289 (3.84), 353 (4.32); $\tilde{\nu}_{max}$(atr)/cm^{-1} 3372 and 2957 (OH), 1756 (C═O), 1679, 1623 and 1606 (C═C), 1445 (CH_3), 1330 (OH), 1272 and 1079 (C–O), 892 and 754 (═C–H); δ_H(500 MHz; DMSO-d_6) 3.85 (3 H, s, OCH_3), 7.31 (1 H, s, 10-H), 7.46 (1 H, ddd, $^3J_{2\text{-H},1\text{-H}}$ 7.4, $^3J_{2\text{-H},3\text{-H}}$ 7.4,$^4J_{2\text{-H},4\text{-H}}$ 1.0, 2-H), 7.54 (1 H, br d, $^3J_{4\text{-H},3\text{-H}}$ 8.4, 4-H), 7.65 (1 H, ddd, $^3J_{3\text{-H},2\text{-H}}$ 7.3, $^3J_{3\text{-H},4\text{-H}}$ 8.3, $^4J_{3\text{-H},1\text{-H}}$ 1.6, 3-H), 7.99 (1 H, dd, $^3J_{1\text{-H},2\text{-H}}$ 7.7, $^4J_{1\text{-H},3\text{-H}}$ 1.4, 1-H); δ_C(125 MHz; DMSO-d_6) 51.87 (OCH_3), 99.35 (C-10), 104.93 (C-6a), 110.76 (C-6b), 112.01 (C-11b), 114.05 (C-7), 116.95 (C-4), 121.38 (C-1), 124.93 (C-2), 131.73 (C-3), 141.69 (C-8), 146.45 (C-9), 148.76 (C-10a), 152.45 (C-4a), 156.57 (C-6), 158.44 (C-11a), 165.97 (CO_2CH_3); *m*/*z*(EI, 70 eV) 326.04335 (M^+, 16%. $C_{17}H_{10}O_7$ requires 326.04266), 294 ($M^+ - CH_4O$, 100), 265 (8), 228 (11), 210 (56), 126 (16), 92 (24), 69 (24), 39 (18).

Acknowledgements

We thank Ms. Sabine Mika for the ^{13}C NMR chemical shift predictions by ACD/Labs and Mr. Matthew Witherspoon for careful consideration of the manuscript.

Notes and references

1 (*a*) A. J. M. da Silva, P. A. Melo, N. M. V. Silva, F. V. Brito, C. D. Buarque, D. V. de Souza, V. P. Rodrigues, E. S. C. Poças, F. Noël, E. X. Albuquerque and P. R. R. Costa, *Bioorg. Med. Chem. Lett.*, 2001, **11**, 283–286; (*b*) H. Wagner, B. Geyer, Y. Kiso, H. Hikino and G. S. Rao, *Planta Med.*, 1986, **52**, 370–373.

2 *PCT Int. Appl.*, WO 2008/110465 A1 20080918.

3 (*a*) H.-W. Wanzlick, R. Gritzky and H. Heidepriem, *Chem. Ber.*, 1963, **96**, 305–307; (*b*) D. Nematollahi and Z. Forooghi, *Tetrahedron*, 2002, **58**, 4949–4953; (*c*) G. Pandey, C. Muralikrishna and U. T. Bhalerao, *Tetrahedron*, 1989, **45**, 6867–6874.

4 (*a*) H. Leutbecher, J. Conrad, I. Klaiber and U. Beifuss, *Synlett*, 2005, 3126–3130; (*b*) H. Leutbecher, S. Hajdok, C. Braunberger, M. Neumann, S. Mika, J. Conrad and U. Beifuss, *Green Chem.*, 2009, **11**, 676–679; (*c*) H. Leutbecher, Ph.D. Thesis, Universität Hohenheim, Stuttgart, Germany, 2007; (*d*) S. Hajdok, H. Leutbecher, G. Greiner, J. Conrad and U. Beifuss, *Tetrahedron Lett.*, 2007, **48**, 5073–5076.

5 (*a*) M. E. Elyashberg, K. A. Blinov, Y. D. Smurnyy, T. S. Churanova and A. J. Williams, *Magn. Reson. Chem.*, 2010, **48**, 219–229; (*b*) K. A. Blinov, Y. D. Smurnyy, T. S. Churanova, M. E. Elyashberg and A. J. Williams, *Chemom. Intell. Lab. Syst.*, 2009, **97**, 91–97; (*c*) S. Thomas, I. Brühl, D. Heilmann and E. Kleinpeter, *J. Chem. Inf. Comput. Sci.*, 1997, **37**, 726–730.

6 (*a*) D. Nematollahi and M. Rafiee, *J. Electroanal. Chem.*, 2004, **566**, 31–37; (*b*) S. S. H. Davarani, N. M. Najafi, S. Ramyar, L. Masoumi and M. Shamsipur, *Chem. Pharm. Bull.*, 2006, **54**, 959–962.

7 ACD/NMR Predictors, V10, Advanced Chemistry Development, Toronto, Canada, 2006.

8 M. J. Frisch, G. W. Trucks, H. B. Schlegel, G. E. Scuseria, M. A. Robb, J. R. Cheeseman, J. A. Montgomery, Jr., T. Vreven, K. N. Kudin, J. C. Burant, J. M. Millam, S. S. Iyengar, J. Tomasi, V. Barone, B. Mennucci, M. Cossi, G. Scalmani, N. Rega, G. A. Petersson, H. Nakatsuji, M. Hada, M. Ehara, K. Toyota, R. Fukuda, J. Hasegawa, M. Ishida, T. Nakajima, Y. Honda, O. Kitao, H. Nakai, M. Klene, X. Li, J. E. Knox, H. P. Hratchian, J. B. Cross, V. Bakken, C. Adamo, J. Jaramillo, R. Gomperts, R. E. Stratmann, O. Yazyev, A. J. Austin, R. Cammi, C. Pomelli, J. Ochterski, P. Y. Ayala, K. Morokuma, G. A. Voth, P. Salvador, J. J. Dannenberg, V. G. Zakrzewski, S. Dapprich, A. D. Daniels, M. C. Strain, O. Farkas, D. K. Malick, A. D. Rabuck, K. Raghavachari, J. B. Foresman, J. V. Ortiz, Q. Cui, A. G. Baboul, S. Clifford, J. Cioslowski, B. B. Stefanov, G. Liu, A. Liashenko, P. Piskorz, I. Komaromi, R. L. Martin, D. J. Fox, T. Keith, M. A. Al-Laham, C. Y. Peng, A. Nanayakkara, M. Challacombe, P. M. W. Gill, B. G. Johnson, W. Chen, M. W. Wong, C. Gonzalez and J. A. Pople, *GAUSSIAN 03 (Revision E.01)*, Gaussian, Inc., Wallingford, CT, 2004.

9 A. M. Sarotti and S. C. Pellegrinet, *J. Org. Chem.*, 2009, **74**, 7254–7260.

10 (*a*) E. K. Kövér, G. Batta and K. Fehér, *J. Magn. Reson.*, 2006, **181**, 89–97; (*b*) R. T. Williamson, B. L. Márquez, W. H. Gerwick and E. K. Kövér, *Magn. Reson. Chem.*, 2000, **38**, 265–273; (*c*) V. Lacerda Jr, G. V. J. da Silva, C. F. Tormena, R. T. Williamson and B. L. Marquez, *Magn. Reson. Chem.*, 2007, **45**, 82–86.

11 (*a*) S. Hajdok, J. Conrad, H. Leutbecher, S. Strobel, T. Schleid and U. Beifuss, *J. Org. Chem.*, 2009, **74**, 7230–7237; (*b*) P. E. Hansen, *Prog. Nucl. Magn. Reson. Spectrosc.*, 1981, **14**, 175–295.

12 I. Fleming, *Grenzorbitale und Reaktionen organischer Verbindungen*, VCH, Weinheim, 1990.
13 (*a*) G. W. Klumpp, *Reaktivität in der organischen Chemie*, Thieme, Stuttgart, 1977; (*b*) R. Sustmann and H. Trill, *Angew. Chem.*, 1972, **84**, 887–888; (*c*) R. Sustmann and R. Schubert, *Angew. Chem.*, 1972, **84**, 888–889.
14 *Chem3D Pro, version 12*, Cambridge Soft, Cambridge, MA, USA, 2009.
15 S. Nicotra, A. Intra, G. Ottolina, S. Riva and B. Danieli, *Tetrahedron: Asymmetry*, 2004, **15**, 2927–2931.
16 S. M. Golabi and D. Nematollahi, *J. Electroanal. Chem.*, 1997, **420**, 127–134.